Journal of Magnetic Resonance **138,** 127–134 (1999)
Article ID jmre.1999.1720, available online at http://www.idealibrary.com on IDEAL®

PFG-ω_1-Filtered TOCSY Experiments for the Determination of Long-Range Heteronuclear and Homonuclear Coupling Constants and Estimation of *J*-Coupling "Crosstalk" Artifacts in 2-D ω_1-Filtered "E. COSY-Style" Spectra

Guangzhao Xu, Bo Zhang, and John Spencer Evans[1,2]

Laboratory for Chemical Physics, New York University, 345 East 24th Street, New York, New York 10010

Received September 25, 1998; revised January 20, 1999

We present novel one- and two-dimensional versions of the ω_1-filtered TOCSY experiment. These experiments utilize pulsed-field gradient techniques and INEPT–reverse INEPT magnetization transfer to generate heteronuclear filtering by means of *coherence pathway selection.* **The major advantages of this approach are twofold: first, each experiment requires a reasonable number of transmitter pulses, gradient pulses, and delays to implement. Second, the use of *z*-axis gradients at the beginning and termination of the pulse sequences prevents the recovery of dephased magnetization prior to FID detection. This technique was incorporated into 1-D and 2-D ω_1-filtered J_{XH}- and J_{HH}-TOCSY-style experiments. As demonstrated on ^{15}N-enriched peptide samples, the use of the pulsed-field-gradient coherence selection scheme effectively filters out unwanted magnetization components, thereby improving the overall sensitivity of the experiments. In addition to this suite of pulse sequences, we also present a method for correcting the reduction in *J*-coupling that results from crosspeak shifting in 2-D ω_1-filtered E. COSY-style spectra. This correction is applicable to both Lorentzian and Gaussian 2-D crosspeak lineshapes.**

Key Words: **pulsed-field gradient; heteronuclear; homonuclear; *J*-coupling; peptides; crosstalk relaxation; isotropic mixing; crosstalk *J*-coupling correction.**

INTRODUCTION

Long-range heteronuclear *J*-couplings ($^{LR}J_{XH}$) can be estimated using heteronuclear half-filtered *J*-resolved experiments (*1, 2*). These experiments are very useful for determining backbone and sidechain torsion angles in polypeptides (*1, 2*). The basic scheme used in these experiments is a proton–proton spin coherence transfer period, in which magnetization transfer occurs between X-bound protons and other protons in the spin coupling network. The resulting spectrum exhibits an E. COSY-style two-dimensional connectivity pattern (*1–3*), where crosspeaks separated by $^1J_{XH}$ in the ω_1 dimension also exhibit frequency displacements equal to $^{LR}J_{XH}$ in the ω_2 dimension. The large $^1J_{XH}$ separation (approximately 140 Hz for ^{13}C, 90 Hz for ^{15}N) makes the displacement measurement independent of crosspeak linewidth and lineshape. The most widely used half-filtered heteronuclear experiment is the 2-D ω_1-filtered TOCSY experiment (*2, 4*). Here, magnetization transfer between X-bound protons and remote protons in the scalar coupling network is accomplished using a spinlock pulse sequence. One dimensional ω_1-filtered TOCSY experiments have also evolved. Here, two 1-D subspectra are obtained by one of the following methods: the paired satellite selection TOCSY method (i.e., PASS-TOCSY) (*5*), or the "in phase–antiphase" method (i.e., IA-TOCSY) (*6, 7*). In these one-dimensional experiments, one observes the $^{LR}J_{XH}$ as a frequency shift in the subspectra (*5–7*). By virtue of their improved digital resolution, these 1-D experiments allow for a more accurate determination of the $^{LR}J_{XH}$, particularly for $^{LR}J_{XH} < 3$ Hz (*5–7*).

Recent studies have reported the use of "excitation sculpting" pulsed-field-gradient (PFG) GBIRD pulse sequences (*8*) for heteronuclear filtering. The GBIRD sequence results in improved heteronuclear filtering capabilities and increased sensitivity in ω_1-filtered TOCSY experiments (*7, 9*). However, these improvements come at a cost: (1) The GBIRD sequence must be applied at the beginning of the pulse sequence (*7–9*). This means that unwanted proton magnetization that is dephased by the GBIRD pulse sequence can recover prior to FID detection. This problem compromises the filtering capabilities of the experiment. (2) For effective filtering, the GBIRD sequence is either employed in a lengthy *n*-cycle format (where $n = 2$ or 4) (*7, 8*) or is combined with other techniques, such as zz-filtering (*9*). Hence, the net ω_1-filtered TOCSY pulse sequence becomes long, rendering it unsuitable for spin systems that experience fast spin–spin relaxation (e.g., large peptides, proteins).

In this report, we present novel one- and two-dimensional versions of the ω_1-filtered TOCSY experiment. We utilize

[1] To whom correspondence should be addressed. E-mail: jse@dave-edmunds.dental.nyu.edu.

[2] Contribution No. 9 from the Laboratory of Chemical Physics, New York University.

1090-7807/99 $30.00

pulsed-field-gradient methods and an INEPT–reverse INEPT magnetization transfer scheme to generate heteronuclear filtering by means of coherence pathway selection (*10, 11*). The major advantages of this approach are twofold: First, each experiment requires a reasonable number of transmitter pulses, gradient pulses, and delays to set up. Second, the use of *z*-axis gradients at the beginning and end of the pulse sequences prevents the recovery of dephased magnetization prior to FID detection. This approach results in a more effective purging of unwanted solute and solvent proton magnetization. The INEPT-style PFG approach was incorporated into two types of experiments: a ω_1-filtered J_{XH}-TOCSY-style experiment (*4, 7, 9*) ($^{LR}J_{XH}$ determination) and a ω_1-filtered J_{HH}-TOCSY-style experiment (*12, 13*) ($^{LR}J_{HH}$ determination). For the ω_1-filtered J_{HH}-TOCSY experiment, the displacement of the cross-peaks in the ω_2 dimension corresponds to a long-range homonuclear coupling (*11, 12*). As demonstrated on ^{15}N-enriched peptide samples, the pulsed-field-gradient coherence selection scheme generates effective heteronuclear filtering within a reasonable pulse sequence timeframe.

In addition to the ω_1-filtered TOCSY pulse sequence schemes, we present an approach for analyzing E. COSY-style *J*-resolved spectra and correcting for "crosstalk" reduction in the observed *J*-coupling. The nature of crosstalk artifacts in E. COSY-style 2-D experiments has been discussed elsewhere (*14, 15*). As shown in this report, the observed shifts in crosstalk-affected E. COSY-style crosspeaks (Lorentzian or Gaussian lineshapes) can be compensated for, and a *J* correction factor can be calculated.

RESULTS AND DISCUSSION

Half-Filtering and "In-Phase–Antiphase" Pulse Sequences

To understand the application of the ω_1-half-filtered TOCSY experiments, we begin with a description of the half-filter and "in-phase–antiphase" coherence selection techniques (Fig. 1A). The heteronuclear half-filter pulse sequence is a PFG-enhanced HSQC-type pulse. The pulse commences with an INEPT-type transfer step (*16, 17*) that generates antiphase coherence for X-bound protons (Fig. 1A). The initial *I*-spin magnetization evolves as $I_y \rightarrow 2I_zS_y$. After the INEPT transfer step, a reverse INEPT transfer step is performed (*18*). Here, the magnetization components evolve as $2I_zS_y \rightarrow I_y$. Hence, using the overall INEPT–reverse INEPT transfer scheme, we retain only one magnetization component, I_y. To achieve selection of coherence pathways, we perform the following steps: (1) apply one *z*-gradient pulse (G_1, during delay t_g) prior to the start of the reverse INEPT transfer step and a second gradient pulse (G_2, during delay t_g) immediately prior to the FID acquisition. (2) Employ nonselective heteronuclear- and proton-180° spin inversion pulses prior to each gradient pulse. The net effect on the spin system is as follows. The G_1 and G_2 dephasing gradients are applied on heteronuclear and proton coherences, respectively. The resulting spatial phase gradients are different multiples of the magnetogyric ratios of the X-nucleus and proton (i.e., γ_S and γ_H) (*10, 11*). By setting the gradient strengths as $G_1{:}G_2 = \pm\gamma_H{:}\gamma_S$, either a "p-type" (when "+" applies) or "n-type" (when "−" applies) coherence (*11, 19*) will be selected, resulting in in-phase detectable magnetization. Protons that are not bound to the X-nucleus are purged from the spectrum by two techniques: dephasing created by the gradient pulses and cycling phases ϕ_1 and ϕ_3 (Fig. 1A). Note that the positioning of the G_2 gradient at the end of the pulse sequence ensures that dephased spins cannot recover before the FID acquisition. Obviously, since one of the two coherence pathways is also dephased by the gradients, the half-filtered experiment suffers from a loss in sensitivity as compared to the GBIRD cycle (*7, 9*). Thus, at the conclusion of the half-filtering experiment, we have heteronuclear-filtered proton magnetization which will experience further evolution according to homonuclear *J*-coupling. There is no active heteronuclear magnetization at this point.

The half-filter pulse sequence outlined above approach differs from the HSQC planar-mixing method (*18, 19*), in which heteronuclear magnetization is active during the t_1 interval. The planar mixing method generates two heteronuclear coherences, $2I_zS_y\cos(\omega_s t_1)$, and, $2I_zS_x\sin(\omega_s t_1)$ (*18, 19*). This second component, $2I_zS_x\sin(\omega_s t_1)$, is retained as a planar component perpendicular to $2I_zS_y\cos(\omega_s t_1)$; both components are refocused at the end of the pulse sequence (*18, 19*). By comparison, the half-filtering pulse sequence described above generates a single magnetization component $2I_zS_y$, and the G_1 gradient pulse generates a magnetization component $2I_zS_x$; these components are *not* mixed and cannot be mixed as per the planar mixing method.

The heteronuclear "in-phase–antiphase" (IA) pulse sequence is created by a simple modification of the half-filtered pulse sequence (Fig. 1A). The last heteronuclear 180° pulse in Fig. 1A is replaced by a $90^\circ_{\phi 4}$–180°_x–$90^\circ_{\phi 4}$ heteronuclear composite pulse sequence (denoted by checkered rectangles). This composite pulse is equivalent to an effective 180° pulse (i.e., "antiphase" magnetization) when $\phi_4 = y$ or an effective 0° pulse (i.e., "in-phase" magnetization) when $\phi_4 = -x$ (*7*). Using the phase cycling protocol and addition/subtraction techniques reported elsewhere (*7*), the resulting satellite peaks appear individually on two separate spectra. The frequency displacement between the two spectra gives rise to the observed *J*-coupling.

J_{XH}- and J_{HH}-TOCSY Pulse Sequences

We create ω_1-filtered TOCSY experiments via simple modification of the pulse sequences shown in Fig. 1A. For example, a 2-D PFG ω_1-filtered J_{XH}-TOCSY experiment can be constructed by appending a t_1 delay and spin–lock at the end of the ω_1-filtered pulse sequence (Fig. 1B). This requires the repositioning of G_2 at the end of the spin–lock sequence to prevent

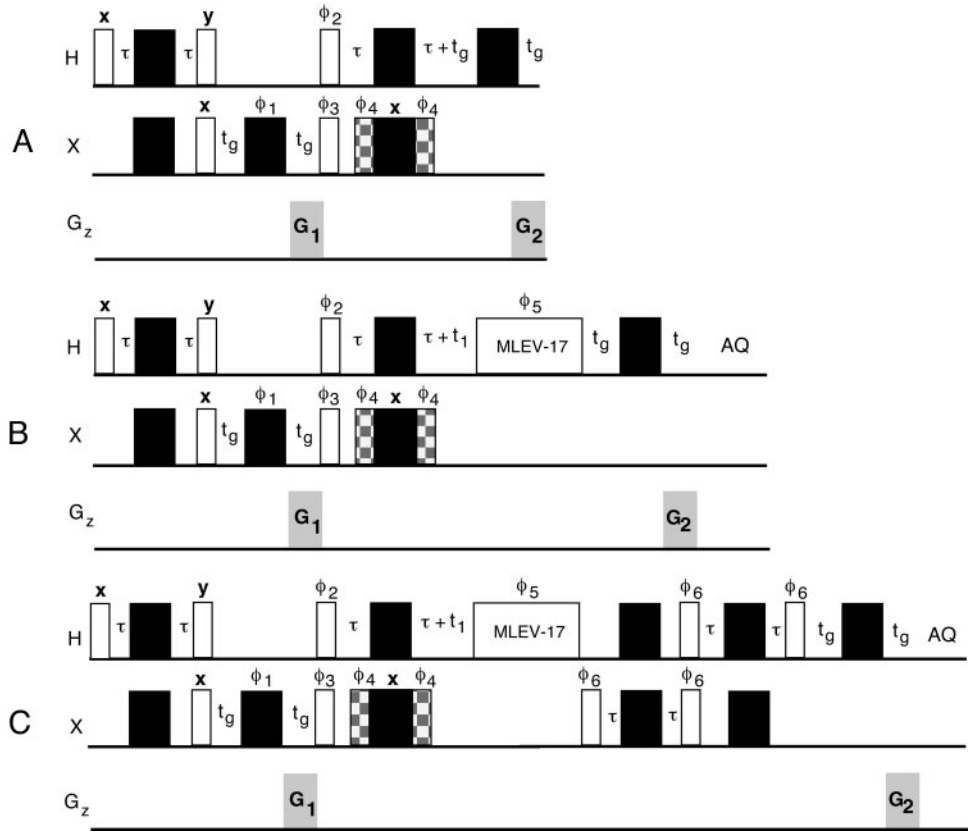

FIG. 1. (A) PFG-ω_1 filtered and "in-phase–antiphase" (IA) coherence transfer pulse sequences. 90° pulse, white rectangles; 180°, black rectangles; "IA" 90°, checkered rectangles. "G", rectangular *z*-gradient RF pulse. Transmitter phases are given above each pulse. Delays: $\tau = \frac{1}{4}\,{}^1J_{XH}$; t_g = duration of gradient pulse + gradient relaxation delay. Note that the "IA" pulses (checkered rectangles flanking black rectangular pulse on the X-nucleus timeline) are *only* utilized in the "IA" experiment. Phase cycling schemes are as follows. For half-filter experiment, $\phi_1 = \{y, y, x, x\}$; $\phi_2 = x$; $\phi_3 = \{x, -x, x, -x\}$; 0ph = $\{x, -x, -x, x\}$. For "IA" experiment, $\phi_1 = \{y, y, x, x\}$; $\phi_2 = x$; $\phi_3 = \{x, -x, x, -x\}$; $\phi_4 = \{y, y, y, y, -x, -x, -x, -x\}$; receiver phase (0ph) = $\{x, -x, -x, x, y, -y, -y, y\}$ for addition experiments or = $\{x, -x, -x, x, -y, y, y, -y\}$ for subtraction experiments. CYCLOPS phase cycling routine is applied on ϕ_2 and 0ph in half-filter and "IA" experiments. (B) PFG-ω_1 filter J_{XH}-TOCSY pulse sequence. The experimental parameters are identical to that given in (A), with ϕ_5 = 0ph. For 1-D version, $t_1 = 0$; for 2-D version, t_1 is incremented as per standard two-dimensional experiment. The hypercomplex scheme is implemented on phases ϕ_2 and 0ph to generate phase-sensitive 2-D spectra. (C) PFG-ω_1 filtered J_{HH}-TOCSY pulse sequence. The experimental parameters are identical to that described in (B), with ϕ_6 = 0ph + 1.

the recovery of dephased magnetization. With the inclusion of the isotropic mixing period and disregarding the effect of gradients on the spin system, we can outline the magnetization evolution for the ω_1-filtered J_{XH}-TOCSY experiment as follows:

$$I_y \xrightarrow{\text{INEPT}} 2I_zS_y \xrightarrow[\text{INEPT}]{\text{Reverse}} I_y \xrightarrow{t_1} I_y\cos(\omega_1 t_1) + iI_x\sin(\omega_1 t_1) \xrightarrow{\text{Spinlock}} I_y^r\cos(\omega_1 t_1) + iI_x^r\sin(\omega_1 t_1) \rightarrow t_2 \quad [1]$$

Here, the superscript r refers to relayed magnetization. A 1-D PFG version (*7*) can be constructed by modifying the 2-D experiment as follows: set the t_1 delay equal to 0 and activate the "IA" sequence as described in the preceding paragraph (Figs. 1A and 1B). In this report, we utilized the "clean" compensated spin–lock sequence to generate isotropic mixing conditions, but one can substitute other suitable composite pulse train sequences for this purpose (e.g., DIPSI (*20*), CABBY (*21*)). The 1-D and 2-D PFG ω_1-filtered J_{HH}-TOCSY experiments (*12, 13*) are similar to the heteronuclear experiment, but require the addition of a [BIRD/2(S) − BIRD/2(H)] composite pulse (*22*) immediately at the end of the spin–lock sequence and before the inversion pulse (Fig. 1C). This composite pulse is similar to the standard BIRD sequence, but here, $\tau = \frac{1}{4}\,{}^1J_{XH}$.

We first test the effectiveness of the ω_1-filter pulse sequence and, subsequently, the "IA" pulse sequence (Fig. 2). The normal one-dimensional proton spectrum (amide fingerprint region) is shown in Fig. 2A. The application of the ω_1-filtered

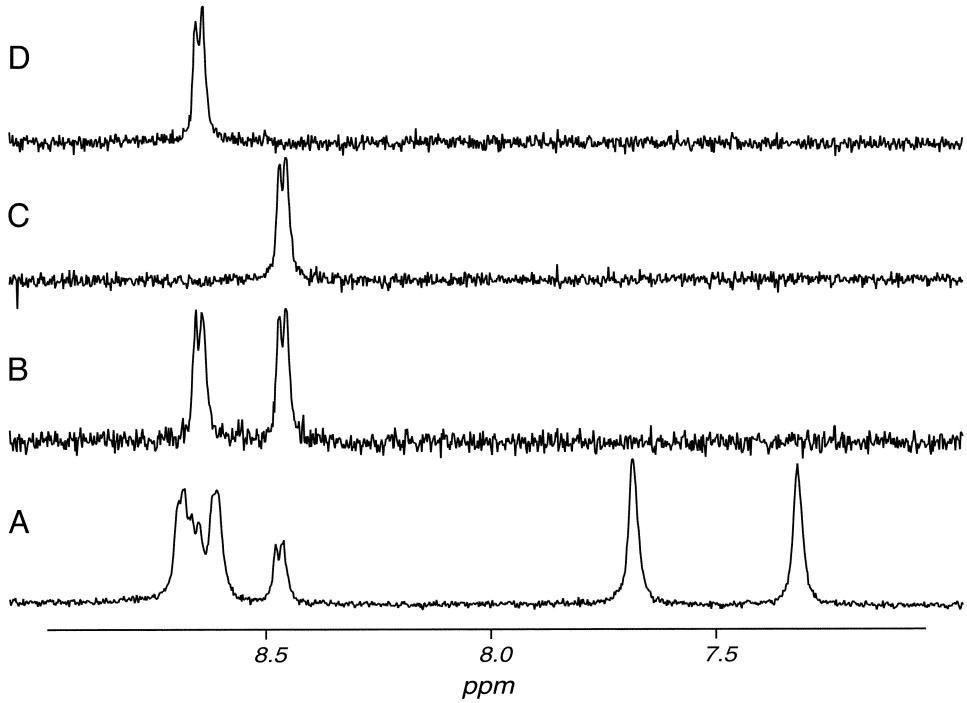

FIG. 2. 1-D NMR PFG-ω_1 filtered and "in-phase–antiphase" experiments (expanded amide fingerprint region). The sample is 10 mM N-α-acetyl-Asp-Val-Asp-C-amide, in 90% v/v H_2O/10% D_2O, 10°C, pH 7.0. The Val residue is ^{15}N-labeled at the α-N position. (A) Normal 1-D spectrum; (B) PFG-ω_1 filtered spectra; (C, D) PFG-ω_1 filtered spectra, with (C) = "in-phase" experiment, (D) = "antiphase" experiment (*6*, *7*). Transmitter pulses: ^{1}H 90° = 10.5 μs, ^{15}N 90° = 42 μs. 64 scans were uitilized for reach spectra. Recovery delay = 1 s. RF *z*-gradient pulses: 1 ms duration, 0.5 ms relaxation time, G_1 = 30 Gauss/cm, G_2 = 3 Gauss/cm. $t = \frac{1}{4}\,{}^1J_{NH}$ with ${}^1J_{NH}$ = 90 Hz. Spectral window was 5200 Hz, and a Lorentzian apodization window function of 2 Hz was applied. Transmitter offset was applied on-resonance with the solvent signal. Proton chemical shifts are referenced from internal d_4-TSP.

"INEPT-style" PFG pulse sequence results in an effective proton filtering of the amide resonances (Fig. 2B). With the application of the IA pulse sequence, we see that only *one* of the two satellite peaks appears on either spectrum (Figs. 2B and 2C), with the frequency displacement equal to the ${}^1J_{NH}$ coupling. Therefore, the gradient-enhanced coherence selection technique does an effective job of purging unwanted proton magnetization from the spectrum.

We next examine the combination of ω_1-filtering and spin–lock coherence transfer steps. As shown in Fig. 3, the 2-D and 1-D PFG ω_1-filtered J_{XH}-TOCSY experiments exhibit effective purging of unwanted proton magnetization. In the 2-D spectrum (Fig. 3A), expansion of the crosspeak region for the Ala ${}^3J_{N-H\beta}$ spin coupling (which relates the χ_1 side chain torsion angle) reveals the expected E. COSY pattern. By measuring the frequency displacement in the ω_2 dimension, we calculate ${}^3J_{N-H\beta}$ = 3.5 Hz. For the 1-D "IA" experiment, expansion of the same frequency region reveals the typical "in-phase–antiphase" displacement (Fig. 3B); here, we obtain a value of 3.4 Hz for ${}^3J_{N-H\beta}$. Note the absence of crosstalk peaks in this spectrum. In Fig. 4, 1-D sections extracted from the amide proton fingerprint region of the 2-D PFG ω_1-filtered J_{XH}-TOCSY also reveal the absence of observable crosstalk peaks. One can assume that, due to the small size of the polypeptide in question, crosstalk phenomena are not observed in either the 1-D or 2-D experiments. The 2-D (Fig. 5A) and 1-D (Fig. 5B) versions of the PFG ω_1-filtered J_{HH}-TOCSY experiment exhibit similar effectiveness and sensitivity. Once again, as shown in Fig. 5B, the 1-D experiment does not exhibit crosstalk artifacts. In Figs. 5A and 5B, the observed frequency displacement represents the Val ${}^3J_{NH-H\alpha}$ coupling (which relates the ϕ torsion angle); we obtain a value of 7.5 Hz for both the 2-D and 1-D experiments, respectively.

Estimation of Crosstalk in Half-Filtered TOCSY Experiments

In the ω_1-filter *J*-resolved experiment, it is assumed that *S* spins do not change their spin states during the *I* spin state isotropic mixing period. Hence, the detected magnetization of the *I* spin states should correlate perfectly with the *S* spin states. However, in E. COSY-style experiments, it has been reported that dipolar relaxation pathways permit "crosstalk" between *S* spin states, which can lead to observed shifts in the E. COSY-like crosspeaks and reduction in observed *J*-coupling constants (*14*). This situation is exacerbated in proteins, where the observed proton linewidths are comparable or greater than the observed *J*-coupling (*14*). One solution to the crosstalk problem is to utilize a spin-state selective (S^3) E. COSY pulse sequence (*14*, *15*) which suppresses crosstalk signals. However, another solution to the crosstalk problem involves the

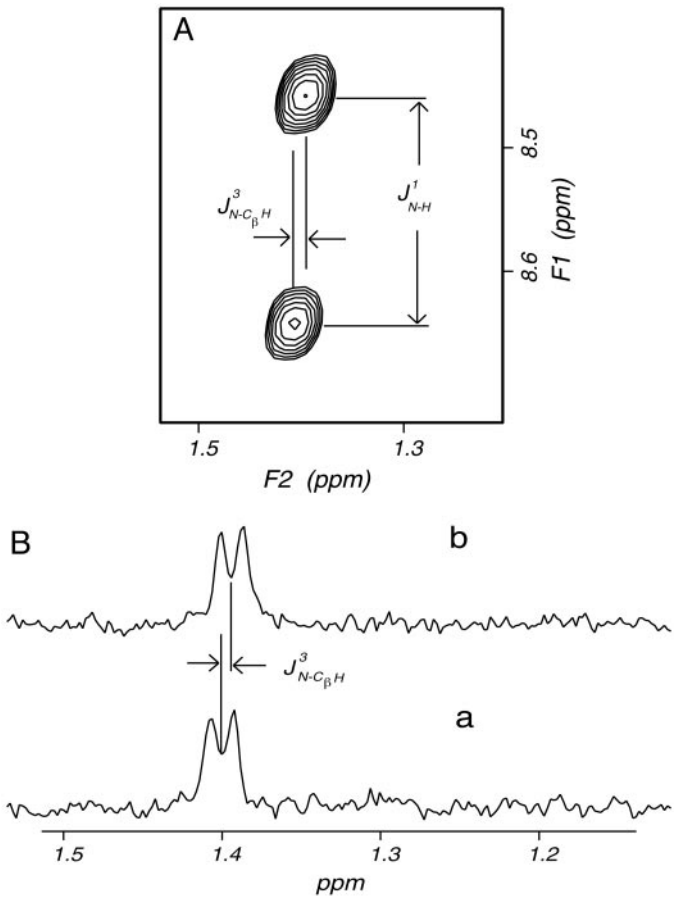

FIG. 3. One- and two-dimensional PFG-ω_1 filtered J_{XH}-TOCSY experiments. The sample is 10 mM N-α-acetyl-Asp-Ala-Asp-C-amide, in 90% v/v H_2O/10% D_2O, 10°C, pH 7.0. The Ala residue is ^{15}N-labeled at the alpha-N position. (A) 2-D ω_1-filtered TOCSY spectra; (B) 1-D "in-phase–antiphase" TOCSY spectra, with (a) "in-phase" experiment, (b) "antiphase" experiment. Both spectra are expanded to show the methyl fingerprint region; transmitter offset was applied on-resonance with the solvent signal. The 2-D spectrum utilized 2048 complex data points in ω_2 dimension, 256 experiments, 64 scans/experiment, spectral window = 5200 Hz, with hypercomplex processing in the ω_1 dimension. For 1-D experiments, 64 scans were utilized, and a Lorentzian apodization window function of 2 Hz was applied. Proton chemical shifts are referenced from internal d_4-TSP.

analysis of the 2-D ω_1-filtered "E. COSY-style" spectra and the correction for the reduction in J-coupling that results from crosspeak shifting. The derivation of this J-coupling correction is detailed in the Appendix; we will briefly summarize the findings here. For two identical crosspeaks with Lorentzian lineshapes (denoted as Peaks 1 and 2), J-coupling adjustment factor, ΔJ, is

$$\Delta J_{\text{Lorentzian}} = 2C_t J^c \frac{1}{[1 + 4\delta^2 (J^c)^2]^2}, \qquad [2]$$

where C_t is the crosstalk probability or intensity term, J^c is the reduced J value due to crosstalk, $\Delta J = J - J^c$, and δ is the inverse of the linewidth. For crosspeaks with Gaussian lineshapes, a similar expression can be derived,

$$\Delta J_{\text{Gaussian}} = 2C_t J^c \exp\left[\frac{-(J^c)^2}{2\sigma}\right], \qquad [3]$$

where σ is the linewidth. For other lineshapes, one can follow the derivation presented in the Appendix to obtain an equivalent expression.

To estimate the adjustment of the J-coupling measurement due to crosstalk relaxation in a given ω_1-filtered TOCSY experiment, we present the following example. As shown below in the hypothetical 2-D spectrum, let us denote the E. COSY-like crosspeak pair ("O") as Peaks 1 and 2, and their corresponding heteronuclear-bound proton peaks as Peaks 3 and 4. In the presence of crosstalk, one should observe minor peaks ("o"), which are denoted as Peaks 3′ and 4′, in the frequency region of Peaks 3 and 4.

$$\begin{array}{ccc} \text{O (3)} & \text{o (4′)} & \text{O (1)} \\ & & \text{F1} \\ \text{o (3′)} & \text{O (4)} & \text{O (2)} \\ & \text{F2} & \end{array} \qquad [4]$$

Note that Peaks 3′ and 4′ are "crosstalk" peaks. The procedure for determining the J correction is as follows: (A) measure the intensity ratio of Peak 3′ to Peak 3, or Peak 4′ to Peak 4. This will yield C_t, or the crosstalk intensity term. (B) Measure the observed J-coupling constant as the chemical shift difference

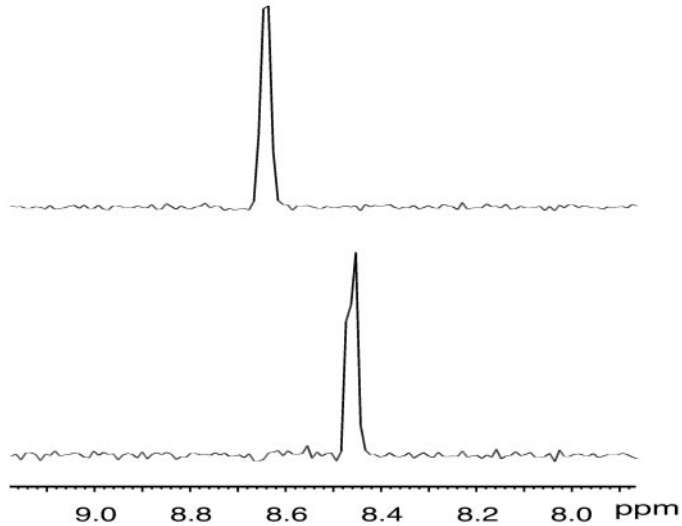

FIG. 4. One-dimensional section (amide proton fingerprint region) from PFG-ω_1 filtered J_{XH}-TOCSY experiment of 10 mM N-α-acetyl-Asp-Ala-Asp-C-α-amide, in 90% v/v H_2O/10% D_2O, 10°C, pH 7.0. Processing parameters utilized here are identical to those for Fig. 3A. These sections were taken parallel to the F1 axis and perpendicular to the F2 axis. Proton chemical shifts are referenced from internal d_4-TSP.

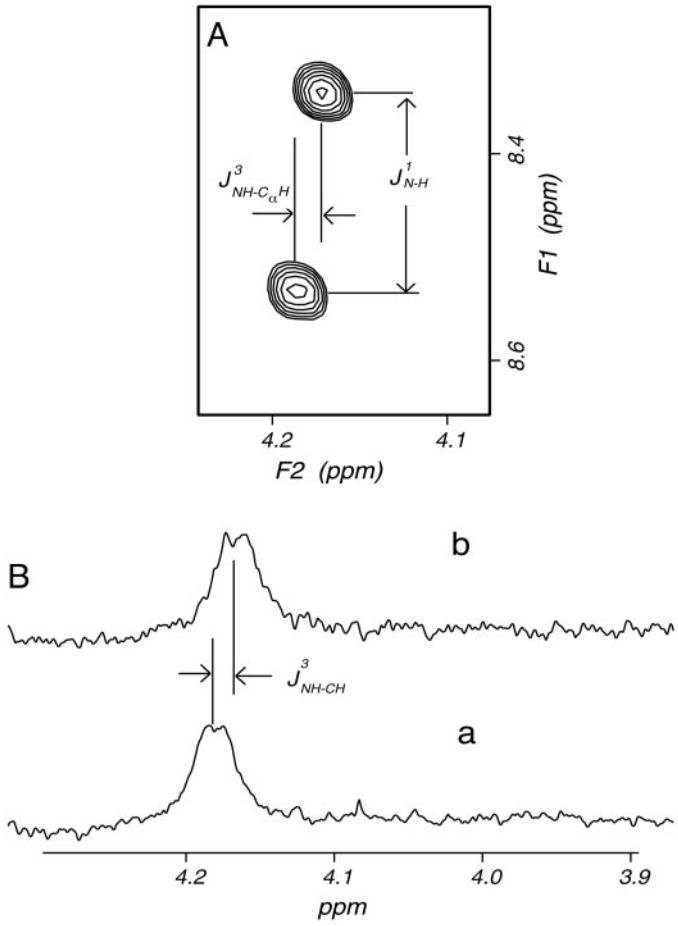

FIG. 5. One- and two-dimensional PFG-ω_1 filtered J_{HH}-TOCSY experiments. The sample is 10 mM N-α-acetyl-Asp-Val-Asp-C-α-amide, in 90% v/v H_2O/10% D_2O, 10°C, pH 7.0. The Val residue is ^{15}N-labeled at the α-N position. (A) 2-D ω_1-filtered TOCSY spectra; (B) 1-D "in-phase–antiphase" TOCSY spectra, with (a) "in-phase" experiment, (b) "antiphase" experiment. Both spectra are expanded to show the α-CH fingerprint region; transmitter offset was applied on-resonance with the solvent signal. Processing parameters are identical to those given in Fig. 3.

between Peaks 1 and 2. This gives the J^c value. (C) Measure the linewidth of Peak 1 or Peak 2, which yields the value of $1/\delta$ in Eq. [2] or σ in Eq. [3]. (D) Depending on the crosspeak lineshape, calculate ΔJ by using Eq. [2] or [3]. The crosstalk "corrected" J-coupling is thus equal to $J^c + \Delta J$.

CONCLUSIONS

In summary, we have designed a suite of one- and two-dimensional PFG-enhanced ω_1-filtered TOCSY experiments for the determination of heteronuclear ($^{LR}J_{XH}$) and homonuclear ($^{LR}J_{HH}$) long-range scalar coupling constants in labeled peptides and proteins. Both experiments utilize the INEPT coherence transfer pulse sequence for ω_1-filtering. The one- and two-dimensional experiments presented herein should be straightforward to implement on most z-axis PFG NMR instruments. Using "clean" isotropic mixing pulse sequences, we note that crosstalk artifacts in the 1-D ω_1-filtered J_{HH}- and J_{XH}-TOCSY spectra and the 2-D ω_1-filtered J_{XH}-TOCSY spectra are suppressed. In addition to the pulse sequences, we present an approach for determining the J-coupling correction for ω_1-filtered E. COSY-style crosspeaks in the presence of crosstalk. This correction is applicable to both Lorentzian and Gaussian 2-D crosspeak lineshapes.

The suite of ω_1-filtered TOCSY experiments offers reasonable resolution and proton filtering capabilities with modest pulse sequence length, which should make them useful tools for determining backbone and sidechain torsion angle preferences for ^{15}N- and/or ^{13}C-labeled peptides and small proteins in solution. The 1-D versions of each TOCSY experiment can be used in situations where small J-coupling determinations are required. Selective excitation versions of each experiment can be created by the substitution of selective bandwidth excitation pulses (e.g., "soft" rectangular, Gaussian, sinc, hypersecant) for the nonselective excitation pulses given in Fig. 1.

EXPERIMENTAL

The pulse sequences were tested on two tripeptides, N$^\alpha$-acetyl-Asp-Val-Asp-C$^\alpha$-amide and N$^\alpha$-acetyl-Asp-Ala-Asp-C$^\alpha$-amide (^{15}N-Val, ^{15}N-Ala, both 98% ^{15}N), both 10 mM in 90% H_2O/10% D_2O, pH 7.0, at 10°C. Both peptides represent triplet Ca (II) binding domains within "acidic" biomineralization mineral recognition proteins (*23, 24*). Experiments were performed on a Varian UNITY-500 spectrometer equipped with a z-gradient driver, using a 5 mm z-axis PFG 3-channel probehead.

APPENDIX

Estimation of Crosstalk and Correction of Observed J Coupling Values

For two "true" crosspeaks (denoted as Peaks 1 and 2) in a 2-D ω_1-filtered TOCSY spectra, the frequency shift of one crosspeak toward the other arises from the presence of crosstalk during the J-coupling experiment. We assume that Peaks 1 and 2 are identical and possess Lorentzian lineshapes; however, we will demonstrate later one that our method can be applied to Gaussian lineshapes as well. We can express the original peak intensities as a function of the frequency

$$g_1(f) = \frac{2T_2}{1 + 4\pi^2 T_2^2 (f - f_1)^2} \quad [5]$$

$$g_2(f) = \frac{2T_2}{1 + 4\pi^2 T_2^2 (f - f_2)^2}, \quad [6]$$

where g_1 and g_2 are the intensities of Peaks 1 and 2 in the absence of crosstalk, T_2 is the transverse spin relaxation time,

and f_1 and f_2 are the Larmor frequencies of Peaks 1 and 2, respectively. The Lorentzian linewidth is given as the quantity, $(\pi T_2)^{-1}$. Let δ be the inverse of the linewidth, i.e., $\delta = \pi T_2$. We can rewrite [5] and [6] as

$$g_1(f) = \frac{1}{1 + 4\delta^2(f - f_1)^2} \quad [7]$$

$$g_2(f) = \frac{1}{1 + 4\delta^2(f - f_2)^2}. \quad [8]$$

Here, the constant $2*T_2$ has been dropped since only the relative intensity is important.

Now, we consider the presence of crosstalk. Peaks 1 and 2 will each receive an overlapping contribution from the minor "crosstalk" Peaks 1′ and 2′. Let us use Peak 1 as an example, and let C_t be the crosstalk probability. Thus, in the presence of crosstalk, the intensity of Peak 1 is

$$g_1^c(f) = \frac{1}{1 + 4\delta^2(f - f_1)^2} + \frac{C_t}{1 + 4\delta^2(f - f_2)^2}, \quad [9]$$

where g_1^c denotes the intensity of Peak 1 in the presence of crosstalk. To find the peak position of g_1^c, we note that, at maximum, the first derivative of $g_1^c = 0$, i.e.,

$$\frac{\partial g_1^c(f_1^c)}{\partial f} = 0. \quad [10]$$

Applying Eq. [10] to Eq. [9], we find that

$$\frac{(f_1^c - f_1)}{[1 + 4\delta^2(f_1^c - f_1)^2]^2} + \frac{C_t(f_1^c - f_2)}{[1 + 4\delta^2(f_1^c - f_2)]^2} = 0, \quad [11]$$

where f_1^c is the Larmor frequency of Peak 1 with crosstalk contributions. Note that

$$f_1^c - f_1 = \frac{1}{2}\Delta J \quad [12]$$

and

$$f_1^c - f_2 = -\frac{1}{2}\Delta J - J^c, \quad [13]$$

where J^c is the reduced J-coupling constant due to crosstalk and $\Delta J = J - J^c$. By substituting Eq. [13] into Eq. [11], we obtain

$$\frac{\Delta J}{[1 + \delta^2\Delta J^2]^2} - \frac{C_t(\Delta J - 2J^c)}{[1 + \delta^2(\Delta J + 2J^c)^2]^2} = 0. \quad [14]$$

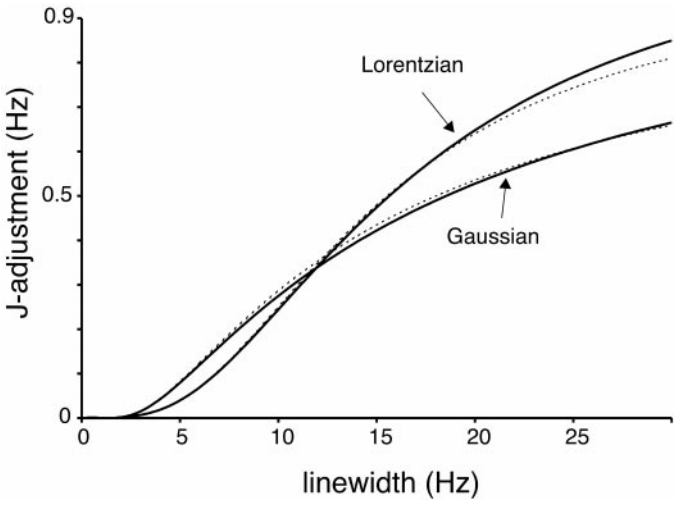

FIG. 6. Calculated corrections (numeric versus formula; Lorentzian versus Gaussian) for the J-coupling due to the crosstalk effect. Solid line, numeric Newton–Raphson solution; Dashed line, formula solution, using values $J^c = 5$ Hz, $C_t = 10\%$.

A similar solution can be derived for the Gaussian lineshape situation. Given the linewidth (i.e., $1/\delta$), J^c, and C_t, ΔJ can be solved numerically from Eq. [14] using a root-searching routine such as a Newton–Raphson approach. However, as described below, we will demonstrate that a simplified formula can be derived to calculate ΔJ.

To arrive at a simplified expression, consider the first term in Eq. [14]. Since ΔJ is small compared to the linewidth, then a reasonable approximation would be that $\delta\Delta J = 0$. Thus, the denominator of the first term in Eq. [14] becomes unity. For the second term in Eq. [14], since $\Delta J \ll 2J^c$, we can approximate the $(\Delta J + 2J^c)$ term as $2J^c$. With these approximations in mind, rearrangement of Eq. [14] yields Eq. [2].

Figure 6 shows calculated corrections (numeric versus formula) for the J-coupling due to the crosstalk effect. In the formula solution, using Eq. [14], J^c was chosen to be 5 Hz, and the crosstalk intensity was assumed to be 10%. These results are plotted against the numeric solution (Newton–Raphson root searching routine) of Eq. [14]. As shown in Fig. 6, the simplified formula gives an acceptable approximation. Note in Fig. 6 that the J-adjustment for Lorentzian and Gaussian lineshapes can differ by approximately 0.2 Hz for linewidths greater than 20 Hz (i.e., arising from large macromolecules such as proteins and nucleic acids) and may vary with J and C_t. However, for small and moderate linewidths (i.e., $<$15 Hz), the difference is smaller than 0.1 Hz, which can be considered negligible since more significant J measurement errors can arise from other sources.

ACKNOWLEDGMENTS

This work was supported in part by grants from the National Science Foundation (Faculty CAREER Award MCB-9513250; MCB-9816703).

REFERENCES

1. P. Schmieder, M. Kurz, and H. Kessler, Determination of heteronuclear long-range couplings to heteronuclei in natural abundance by two- and three-dimensional NMR spectroscopy, *J. Biomol. NMR* **1,** 403–420 (1991).
2. P. Schmieder and H. Kessler, Determination of the Phi angle in a peptide backbone by NMR spectroscopy with a combination of homonuclear and heteronuclear coupling constants, *Biopolymers* **32,** 435–440 (1992).
3. L. Muller, P.E.COSY, a simple alternative to E-COSY, *J. Mag. Res.* **72,** 191–196 (1987).
4. M. Kurz, P. Schmieder, and H. Kessler, HETLOC, an efficient method for determining heteronuclear long range coupling with heteronuclear in natural abundance, *Angew. Chem.* (Int. Ed., English) **30,** 1329–1331 (1991).
5. R. Bazzo, G. Barbato, and D. O. Cicero, Accurate measurement of heteronuclear long-range coupling constants from 1D subspectra in crowded spectral regions, *J. Magn. Reson. Series A* **117,** 267–271 (1995).
6. D. Yang and K. Nagayama, A sensitivity-enhanced method for measuring heteronuclear long-range coupling constants from the displacement of signals in two 1D subspectra, *J. Magn. Reson. Series A* **118,** 117–121 (1996).
7. G. Xu and J. S. Evans, Determination of long-range J_{XH} couplings using "excitation sculpting" gradient-enhanced heteronuclear correlation experiments, *J. Magn. Reson. Series A* **123,** 105–110 (1996).
8. G. Maklin and A. J. Shaka, Phase-sensitive two-dimensional HMQC and HMQC-TOCSY spectra obtained using double pulsed-field gradient spin echoes, *J. Magn. Reson. Series A* **118,** 247–255 (1996).
9. D. Uhrin, G. Batta, V. J. Hruby, P. N. Barlow, and K. E. Kover, Sensitivity- and gradient-enhanced hetero (ω_1) half-filtered TOCSY experiment for measuring long-range heteronuclear coupling constants, *J. Magn. Reson.* **130,** 155–161 (1998).
10. P. B. Barker and R. J. Freeman, Pulsed field gradients in NMR, an alternative to phase cycling, *J. Magn. Reson.* **64,** 334–338 (1985).
11. R. E. Hurd and B. K. John, Gradient-enhanced proton-detected heteronuclear multiple-quantum coherence spectrocopy, *J. Magn. Reson.* **91,** 648–653 (1991).
12. W. Williker and D. Leibfritz, Accurate measurement of homonuclear coupling constants using JHH TOCSY, *J. Magn. Reson.* **99,** 421–425 (1992).
13. W. Williker and D. Leibfritz, A selective JHH TOCSY version for measuring $^3J_{HH}$ coupling constants, *J. Magn. Reson. Series A* **110,** 95–97 (1994).
14. A. Meissner, T. Schulte-Herbruggen, and O. W. Sorensen, Relaxation artifacts and their suppression in multidimensional E. COSY-type NMR experiments for measurement of J coupling constants in ^{13}C- or ^{15}N-labeled proteins, *J. Am. Chem Soc.* **120,** 7989–7990 (1998).
15. A. Meissner, J. O. Duus, and O. W. Sorensen, Spin-state-selective excitation. Application for E. COSY-type measurement of J_{HH} coupling constants, *J. Magn. Reson.* **128,** 92–97 (1997).
16. G. A. Morris, Sensitivity enhancement in ^{15}N NMR. Polarization transfer using INEPT pulse sequence, *J. Am. Chem. Soc.* **102,** 428–429 (1990).
17. G. A. Morris and R. Freeman, Enhancement of nuclear magnetic resonance signals by polarization transfer, *J. Am. Chem. Soc.* **101,** 760–762 (1990).
18. J. Cavanagh, A. G. Palmer III, P. E. Wright, and M. Rance, Sensitivity improvement in proton-detected two-dimensional heteronuclear relay spectroscopy, *J. Magn. Reson.* **91,** 429–436 (1991).
19. L. Kay, P. Keifer, and T. Saarinen, Pure absorption gradient enhanced heteronuclear single quantum correlation spectroscopy with improved sensitivity, *J. Am. Chem. Soc.* **114,** 10663–10665 (1992).
20. J. Cavanaugh and M. Rance, Suppression of cross-relaxation effects in TOCSY spectra via a modified DIPSI-2 mixing sequence, *J. Magn. Reson.* **96,** 670–678 (1992).
21. J. Quant, T. Prasch, S. Ihringer, and S. J. Glaser, Tailored correlation spectroscopy for the enhancement of fingerprint cross peaks in peptides and proteins, *J. Magn. Reson. Series B* **106,** 116–121 (1995).
22. C. Griesinger, H. Schwalbe, J. Schleucher, and M. Sattler, *in* "Two Dimensional NMR Spectroscopy" (W. R. Croasmun and R. M. K. Carlson, Eds.), p. 509, VCH, Weinheim/New York, 1994.
23. H. A. Lowenstam, S. Weiner, *in* "On Biomineralization," pp. 5–89, Oxford Univ. Press, New York, 1989.
24. J. S. Evans, T. Chiu, and S. I. Chan, Phosphophoryn, a biomineralization template protein. Conformational folding in the presence of Cd (II), *Biopolymers* **34,** 1027–1036 (1994).